A new single-step mechanism for hydrogen combustion

Alejandro Millán-Merino, Pierre Boivin

A new single-step mechanism for hydrogen combustion

Alejandro Millán-Merino[a,b,*], Pierre Boivin[c]

[a] *Universidad Politécnica de Madrid, Madrid, Spain*
[b] *Dept. Ingeniería Térmica y de Fluidos, Universidad Carlos III de Madrid, Leganés, Spain*
[c] *Aix Marseille Univ, CNRS, Centrale Marseille, M2P2, Marseille, France*

Abstract

A single-step chemical-kinetic mechanism is developed that provides good predictions of laminar burning velocities and auto-ignition times. Reasonably accurate adiabatic flame temperatures and (consequently) total amounts of heat release are first obtained through asymptotic expansions of equilibrium expressions for the production of H, O, and OH radicals from the stable products, H_2O along with H_2 and O_2. By ignoring the inner flame structure, this yields minimal computational stiffness for a wide range of equivalence ratios and pressures. In the single-step rate expression, a passive scalar carrying the radical pool is then introduced that enables reasonable laminar flame structures and burning velocities to be calculated. An additional passive scalar measuring pre-heat-release radical build-up serves to track auto-ignition properly as well, thereby providing reasonable predictions for time-dependent as well as steady-state conditions. The results from this computationally convenient formulation are useful for describing a number of combustion processes, including counter-flow flames.

*Corresponding author
Email address: al.millan@upm.es (Alejandro Millán-Merino)

Keywords: Hydrogen, combustion, reduced chemistry

Novelty and significance statement

Hydrogen combustion plays a key role in the carbon-free energy transition. The CPU cost/accuracy balance between detailed and reduced chemistries makes it hard to get the full approval of the CFD community. This balance is more likely in single-step mechanisms due to errors in flame temperature predictions and narrow application conditions. In this study, we apply the novel formalism of varying stoichiometric coefficients to construct a single-step mechanism that accurately reproduces adiabatic temperatures. A global reaction rate constructed from the flame chain-branching analysis and the flammability limits is proposed. Furthermore, an optional passive scalar coupling is presented to extend the capabilities of the present mechanism to autoignition predictions. This work provides an efficient and accurate alternative scheme for CFD hydrogen combustion applications, valid for a wide range of conditions.

CRediT authorship contribution statement

A. Millán-Merino: Conceptualization, Methodology, Software, Writing. **P. Boivin:** Formal analysis, Writing.

Introduction

Accurate and robust reduced chemistry descriptions are fundamental for numerical simulations of complex reactive flow configurations. For hydrogen, reduction may seem futile as the number of chemical species present in the

detailed descriptions (8 reactive + inert species) is relatively small and easily manageable by numerical solvers.

Yet, a large number of reduced chemistry mechanisms for hydrogen chemistry have been proposed in the past [1–7]. Peters et al. proposed a 2-step reduced mechanism [1] assuming each intermediary species but H-atom to be in quasi-steady-state approximation. The 2-step mechanism yields reasonable accuracy for flame propagation velocities. Boivin et al. [6, 7] proposed a 3-step mechanism retaining in addition HO_2, H_2O_2 or a hybrid species accounting for both, to extend the mechanism's application to diffusion flames and autoignition.

Yet, these 2-3 steps reduced descriptions have not gained the full approval of the CFD community, which often prefers the use of skeletal descriptions upon which the reduced mechanisms are built. For instance, the 12-step skeletal description of Boivin [6] has gained far more popularity for complex numerical simulations [8, 9], than its 3-step reduced counterpart.

For the community to adopt reduced chemistry – if need be – the compromise CPU cost/accuracy has to be positive, a hard bargain when only a few species are available to be neglected (contrary to hydrocarbons detailed chemistry, which sometimes includes hundreds of chemical species).

Another interesting way of reducing the CPU cost associated with the chemistry integration is to reduce its stiffness. This is hard to achieve with 2-3 reduced descriptions: the descriptions still involve an intermediate species (typically H or OH) associated with short time scales in the flame and yielding the stiffness.

An obvious way to alleviate this stiffness is removing altogether interme-

diate species and their associated maximum in the flame structure. Many approaches appear in the literature to construct a 1-step mechanism: extending the quasi-steady-state approximations to H-radical [10–12], fitting the Arrhenius parameters of a global reaction rate [13–16], or relying on tabulated Arrhenius coefficients [17, 18]. However, it is known that 1-step H_2 descriptions, typically involving the global hydrogen oxidation step $2\,H_2 + O_2 \longrightarrow 2\,H_2O$ yield awful adiabatic temperature descriptions, discarding them for most practical applications. This error is related to the H/O/OH species being in significant quantities in the burnt gases via dissociation reactions: their positive formation enthalpies significantly decrease the final temperature and must be taken into account to predict the heat release.

The present study offers an intermediate option, building upon a recent 1-step reduced description for (arbitrary) hydrocarbon combustion [19]. A single-step mechanism for H_2 combustion is proposed, effectively diminishing the system stiffness (each species being now monotonous from fresh to burnt states), whilst keeping H/O/OH species to predict very accurately adiabatic temperatures.

The paper is organized as follows. Section 1 presents a new analytical prediction of the thermo-chemical equilibrium from any possible initial state. Knowledge of this equilibrium everywhere allows to introduce a 1-step chemistry with varying stoichiometric parameters designed to reach exactly the local thermo-chemical equilibrium. The rate of the production is then analytically derived in Section 2, and the mechanism is validated for laminar flame propagation velocities. Section 3 presents and validates a simple way to accurately reproduce autoignition - in addition to premixed flames -

without altering the flame propagation results or the description's stiffness. Finally, the mechanism is tested for counterflow diffusion flames in Sec. 4 and conclusions are drawn in Sec. 5.

1. Asymptotic analysis of the equilibrium

This contribution pertains to an ideal-gas mixture of hydrogen and oxygen with diluents. The initial number of moles of the ith species is defined as n_i^0. For example for hydrogen-air mixtures, $n_{\mathrm{H_2}}^0 = \phi$, the equivalence ratio, if $n_{\mathrm{O_2}}^0 = \frac{1}{2}$, and $n_{\mathrm{N_2}}^0 = \frac{1}{2}\frac{79}{21}$. The simplest equilibrium approximation consists of assuming total oxidation,

$$\mathrm{H_2} + \frac{1}{2}\,\mathrm{O_2} \xrightarrow{\xi_1} \mathrm{H_2O}, \tag{1}$$

where ξ_1, the molar advancement of reaction (1), is a helpful normalized measure of the extent to which the reaction has proceeded to produce the product. Its value, zero when there is no product, is less than the maximum value ξ_1^m given by

$$\xi_1^m = \min\left(\phi, 1\right), \tag{2}$$

the limit (2) accounting for the influence of excess oxygen in the mixture if the equivalence ratio is less than unity, with fuel in the mixture otherwise, and

$$\phi = \frac{1}{2}\frac{n_{\mathrm{H_2}}^0}{n_{\mathrm{O_2}}^0} \tag{3}$$

corresponds to the associated equivalence ratio. In this case, the equilibrium composition is fully characterized by $n_i = n_i^0 + \xi_1^m \nu_{1,i}$, and the molar advancement is limited by the deficient reactant. The equilibrium temperature and

pressure can be computed from classical thermodynamic assumptions (e.g. constant pressure and enthalpy or constant volume and internal energy).

1.1. Leading-order prediction

The assumption of complete combustion to H_2O provides a good approximation at normal atmospheric initial conditions when the concentration of one of the reactants is much higher than that of the other, but when the concentrations of both reactants are comparable it overpredicts the extent of reactant consumption greatly, and unreasonably high equilibrium temperatures are obtained. To correct that error, thermodynamic equilibrium needs to be considered, with atom conservation employed to relate the species concentrations to the equivalence ratio. When the chemistry is described by the global reaction (1), the equilibrium condition may be expressed as

$$K_1 = \frac{n^0_{\mathrm{H_2O}} + \xi_1}{\phi - \xi_1} \sqrt{\frac{2N^0 - \xi_1}{1 - \xi_1}}, \tag{4}$$

where

$$K_1 = \exp\left(\frac{g_{H_2} + g_{O_2}/2 - g_{H_3O}}{\mathcal{R}T}\right)\sqrt{P} \tag{5}$$

is the equilibrium constant for reaction (1), g_i being the molar Gibbs function of the $\mathrm{i^{th}}$ species and $\mathcal{R}$ the ideal gas constant, and the equilibrium temperature and pressure are T and P, respectively. Here $N^0 = \sum_{i=1}^{N_s} n_i^0$ denotes the initial total number of moles.

Equation (4) is a third-order polynomial with either three real roots or one plus a complex-conjugate pair. Restricting the solution for ξ_1 to the one that produces positive values of mole numbers for all the species, ξ_1 takes

the value

$$\xi_1 = \frac{1}{3(K_1^2-1)} \min \begin{cases} \alpha + \left(\gamma + \frac{\alpha^2-\beta}{\gamma}\right) \cos\left(\frac{\theta}{3}\right) \\ \alpha + \left(\gamma + \frac{\alpha^2-\beta}{\gamma}\right) \cos\left(\frac{\theta+2\pi}{3}\right) \end{cases} \tag{6}$$

where the following definitions have been introduced for convenience:

$$\alpha = (2\phi+1)K_1^2 + 2n^0_{\mathrm{H_2O}} - 2N^0 \tag{7}$$

$$\beta = \left[(\phi^2+2\phi)K_1^2 + (4N_0 - n^0_{\mathrm{H_2O}})n^0_{\mathrm{H_2O}}\right] 3(K_1^2-1) \tag{8}$$

$$\gamma = \begin{cases} \sqrt[3]{\left|\frac{\sigma}{2} + \sqrt{\Psi}\right|}, & \text{if } \Psi \geq 0 \\ \sqrt{\alpha^2-\beta}, & \text{if } \Psi < 0 \end{cases} \tag{9}$$

$$\theta = \begin{cases} \mathrm{atan2}(0, \frac{\sigma}{2} + \sqrt{\Psi}), & \text{if } \Psi \geq 0 \\ \mathrm{atan2}(\sqrt{-\Psi}, \frac{\sigma}{2}), & \text{if } \Psi < 0 \end{cases} \tag{10}$$

$$\Psi = \frac{\sigma^2}{4} + \left(\beta - \alpha^2\right)^3 \tag{11}$$

$$\sigma = a_3 K_1^6 + 3a_2 K_1^4 + 3a_1 K_1^2 + a_0 \tag{12}$$

with the coefficients a_i defined as:

$$\begin{cases} a_3 & = -2(\phi-1)^3 \\ a_2 & = \phi^2(6\phi-3) + 6\phi \\ & \quad + n^0_{\mathrm{H_2O}}\left[n^0_{\mathrm{H_2O}}(6\phi+3) + \phi(10\phi+4) + 4\right] \\ & \quad - 2N^0\left[(2\phi + 3n^0_{\mathrm{H_2O}} + 1)^2 + (\phi-1)^2\right] \\ a_1 & = n^0_{\mathrm{H_2O}}\left[n^0_{\mathrm{H_2O}}(6n^0_{\mathrm{H_2O}} + 10\phi + 5) + 6\phi(\phi+2)\right] \\ & \quad - 2N^0\left[\phi(4n^0_{\mathrm{H_2O}} + 3\phi + 6) + 3n^0_{\mathrm{H_2O}}(1 - n^0_{\mathrm{H_2O}})\right] \\ & \quad + 8\left(N^0\right)^2(2\phi + 3n^0_{\mathrm{H_2O}} + 1) + 9\phi^2 \\ a_0 & = -2\left(n^0_{\mathrm{H_2O}} + 2N^0\right)^3 \end{cases} \tag{13}$$

based on the initial species concentration. This solution recovers the complete-combustion limit when one reactant is dominant ($n^0_{H_2} \gg n^0_{O_2}$ or $n^0_{H_2} \ll n^0_{O_2}$).

1.2. Influences of radical equilibrium

While the preceding results provide reasonable estimates of the adiabatic flame temperature and associated concentrations for flames in mixtures initially at normal atmospheric conditions, in practical applications fresh gases are usually compressed before their injection in the combustion chamber. The resulting conditions of pressure and temperature yield additional species in the product-gas composition. For hydrogen-air mixtures, the additional species that have to be considered to evaluate the correct burnt-gas temperature are OH, H, and O. These species can be included by considering the following dissociation/recombination reactions:

$$H_2O \xrightarrow{\xi_2} \frac{1}{2}H_2 + OH \tag{14}$$

$$\frac{1}{2}H_2 \xrightarrow{\xi_3} H \tag{15}$$

$$\frac{1}{2}O_2 \xrightarrow{\xi_4} O. \tag{16}$$

Equations (14)-(16) are listed in the order of their contribution to the burnt-gas temperature. At moderate temperatures equations (15) & (16) have a negligible effect on the adiabatic flame temperature, but their contribution increases as the initial condition becomes hotter. Radical product concentrations can be estimated by considering equilibrium conditions for these three dissociation reactions. In general, when these equations are coupled with (4) the resulting system of equations needs to be solved numerically. However, to a large extent, the major-species concentrations are unaffected

by the dissociation reactions. With the assumption that those concentrations are unchanged, the equilibrium conditions for the dissociation equations provide an explicit solution for the molar advancement (bounded by zero and unity) of each additional species, namely

$$\xi_2 = K_2(n^0_{\mathrm{H_2O}} + \xi_1)\sqrt{\frac{N^0 - \frac{\xi_1}{2}}{\phi - \xi_1}} - n^0_{\mathrm{OH}} \tag{17}$$

$$\xi_3 = K_3\sqrt{(\phi - \xi_1)\left(N^0 - \frac{\xi_1}{2}\right)} - n^0_{\mathrm{H}} \tag{18}$$

$$\xi_4 = \frac{K_4}{2}\sqrt{(\phi - \xi_1)(2N^0 - \xi_1)} - n^0_{\mathrm{O}}. \tag{19}$$

Including the products HO_2 and H_2O_2 has very minor effects on equilibrium temperatures under all conditions. Figure 1 compares predictions for initial conditions of 300 K and 1 atm (top) and of isentropic compression from that normal condition to 100 atm (bottom).

As described for hydrocarbon combustion in [19], the equilibrium temperature is needed to compute equilibrium constants, e.g. eq. (5). In the present work, a procedure is proposed to achieve converge to the burnt-gas temperature efficiently: An initial estimate of T is selected considering complete combustion eqn. (2), then a simple Newton-Rahpson method is used to converge on the equilibrium temperature and concentrations, with the Jacobian matrix evaluated numerically. This procedure was found to require no more than 4 iterations (in the worst-case scenario) to converge within a relative tolerance lower than 0.1%.

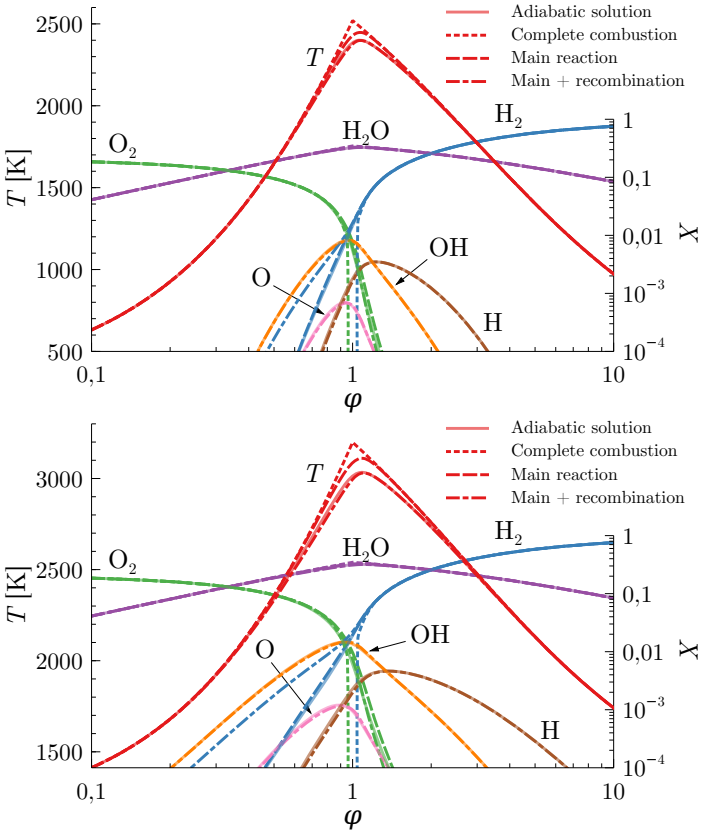

Figure 1: Equilibrium temperature and molar fractions for H_2-air mixtures as functions of the equivalence ratio at 1 and 100 bar (from top to bottom). Solid curves: equilibrium, from Cantera. Dotted curves: complete depletion of reactants. Dashed curves: only the main reaction solution ξ_1 (6). Dash-dot curves: the main reaction along with recombination reactions. (17)-(19).

2. Kinetic mechanism and laminar burning velocities

A global one-step mechanism may be written as

$$\nu'_{\mathrm{H}}\mathrm{H}_2 + \nu'_{\mathrm{O}}\mathrm{O}_2 \xrightarrow{\omega} \nu'_{\mathrm{H_2O}}\mathrm{H_2O} + \nu'_{\mathrm{OH}}\mathrm{OH} + \nu'_{\mathrm{H}}\mathrm{H} + \nu'_{\mathrm{O}}\mathrm{O} \tag{20}$$

where the stoichiometric coefficient of the global equation (20) for the ith species is defined as

$$\nu'_i = 2\sum_{k=1}^{4} \frac{\xi_k}{\xi_1^m}\nu_{k,i}, \tag{21}$$

where the molar advancement of the elementary reaction kth is computed from the local equilibrium predictions as described in section 1 from local pressure and enthalpy estimates. This selection ensures that a correct burnt-gas temperature will be achieved, independent of the reaction rate imposed, ω, which then plays a role only in determining kinetic properties of interest, such as the laminar flame propagation velocity, V_L.

Many previously cited studies [20] have shown that classical Arrhenius expressions

$$\omega = C_{\mathrm{H_2}} C_{\mathrm{O_2}} B e^{-T_a/T}$$

are not suitable for describing H_2-air mixtures, in contrast to hydrocarbon combustion [19, 21, 22]. The values of B and T_a fitted to match V_L computations can apply only over a narrow range of initial conditions, and they need to be recomputed for different scenarios. Alternative formulations that are based on quasi-steady-state assumptions (QSSa) need, as a minimum, a 2-step mechanism for a generally valid global description, although a 1-step description may apply when the application is limited to being close to the flammability limits [11, 20].

It is helpful to base the discussion on the multipurpose 12-step skeletal mechanism of P. Boivin et al. [6]; see table 1, where the steps needed for various purposes are identified in the columns at the right. Reduced mechanisms for V_L (1-step and 2-step) agree on the elementary reactions, do not involve HO_2 and H_2O_2, and differ only in the QSSa applied to the intermediate species. In contrast, mechanisms developed for ignition delay times (τ_{ig}) [23] must include low-temperature chemistry that involves HO_2 and H_2O_2, which have a negligible effect on V_L. Additionally, in the τ_{ig} mechanisms a correct prediction of the burnt-gas temperature is not needed, leading to shorter mechanisms consisting of irreversible reactions, while the irreversible reactions 1-6 correspond to the minimum set of reactions required for the flame-propagation velocity (the λ^+ column), but 8 and 9 are necessary to achieve correct burnt-gas temperatures and compositions.

Tab. 1 also introduces the definitions of reaction forward/backward inverse characteristic times (l_{if}, l_{ib}), used throughout the reduced mechanism derivation.

2.1. One-step QSSA chemistry

In the lean and rich limits, it was shown that a single step chemistry $2\,H_2 + O_2 \longrightarrow 2\,H_2O$ using the first 9 reactions of Tab. 1 was sufficient to accurately recover flame velocities [11]. Assuming H, O and OH steady states, the reaction rate reads

$$\omega = \omega_{4f} + \omega_{8f} + \omega_{9f} = k_{4f} C_{M_4} C_{O_2} C_H + k_{8f} C_{M_8} C_{OH} C_H + k_{9f} C_{M_9} C_H^2, \quad (22)$$

with steady-state expressions required for H and OH being fully explicit [11].

	Reaction	V_L^{a}	$\tau_{\mathrm{ig}}^{\mathrm{b}}$	l_{if}	l_{ib}
1	$\mathrm{H + O_2 \rightleftharpoons OH + O}$	f-b	f	$C_{\mathrm{O_2}} k_{1f}$	–
2	$\mathrm{H_2 + O \rightleftharpoons OH + H}$	f-b	f	$C_{\mathrm{H_2}} k_{2f}$	–
3	$\mathrm{H_2 + OH \rightleftharpoons H_2O + H}$	f-b	f	$C_{\mathrm{H_2}} k_{3f}$	$C_{\mathrm{H_2O}} k_{3b}$
4	$\mathrm{H + O_2 + M \longrightarrow HO_2 + M}$	f	f	$C_{\mathrm{O_2}} C_{\mathrm{M_4}} k_{4f}$	–
5	$\mathrm{HO_2 + H \longrightarrow 2\,OH}$	f	-	$C_{\mathrm{HO_2}} k_{5f}$	–
6	$\mathrm{HO_2 + H \rightleftharpoons H_2 + O_2}$	f	b	$C_{\mathrm{HO_2}} k_{6f}$	–
7	$\mathrm{HO_2 + OH \longrightarrow H_2O + O_2}$	f	-	$C_{\mathrm{HO_2}} k_{7f}$	–
8	$\mathrm{H + OH + M \rightleftharpoons H_2O + M}$	f-b	-	–	–
9	$\mathrm{2\,H + M \rightleftharpoons H_2 + M}$	f-b	-	–	–
10	$\mathrm{2\,HO_2 \longrightarrow H_2O_2 + O_2}$	-	f	–	–
11	$\mathrm{HO_2 + H_2 \longrightarrow H_2O_2 + H}$	-	f	–	–
12	$\mathrm{H_2O_2 + M \longrightarrow 2\,OH + M}$	-	f	–	–

Table 1: The 12-step skeletal mechanism of P Boivin et al. [6] for hydrogen combustion. Columns V_L and τ_{ig} represent elementary reactions involved in laminar-flame propagation velocities [11] and ignition delay times [23]. Columns (l_{if}, l_{ib}) include definitions for inverse characteristic time of the i^{th} forward/backward reaction. Note that the forward/backward subscript f/b may be omitted when either reaction is neglected in Tab. 1.

For the sake of the discussion, let us only consider here the lean/rich limit formulas for ω, also provided in [11].

$$\omega = \begin{cases} \omega_l &= \left(\frac{l_1}{l_4} - 1\right) \frac{l_2 l_{3f}/k_{1b}}{1 + l_{3b}/l_4} \quad \text{in the lean limit} \\ \omega_r &= \left(\frac{l_1}{l_4} + \frac{k_{5f}}{k_{5f} + k_{6f} + k_{7f} \frac{l_{3b}}{l_{3f}}} - 1\right) \frac{l_4^2}{\frac{l_{3b}}{l_{3f}} k_{8f} + k_{9f}} \quad \text{in the rich limit} \end{cases} \tag{23}$$

As expected, the lean formula depends on the $\mathrm{H_2}$ concentration ($l_2 l_{3f} \sim C_{\mathrm{H_2}}^2$)

– the limiting reactant – while the rich limit depends on the O_2 concentration ($l_4^2 \sim C_{O_2}^2$).

In [11] it was shown that the above mechanism yields excellent agreement for all pressure, in both lean and rich limits. This will serve as the basis for the next Section.

Note that a continuous formula valid from lean to rich mixtures was also derived [11], but the resulting flame velocities are not satisfactory at low pressures, as shown later (but they yield good predictions at high pressure).

In the lean limit, it is clear that the reaction term ω_l vanishes when

$$\omega_{1f} = \omega_{4f}, \tag{24}$$

corresponding the lean crossover condition for premixed hydrogen-air flames [11, 24]. In the rich limit, the crossover condition is modified as

$$\omega_{1f} = \omega_{4f} \left(1 - \frac{k_{5f}}{k_{5f} + k_{6f} + k_{7f} \frac{l_{3b}}{l_{3f}}} \right). \tag{25}$$

The following subsection attempts to better approximate the reaction rate without assuming H/O/OH steady states in approximating the H to OH and H to O ratios in the radical pool.

2.2. A study of the chain-branching in flames

Let us delve deeper into the chain-branching region of the flame, close to the crossover temperature, to better approximate the H to OH ratio in the radical pool. Out of the 9 steps identified for flames, the reverse of steps 1, 2 and 3 may be neglected since they each involve two minor (intermediate or product species). For the same reason, recombination steps 8 and 9 are

negligible. There is no need to discard steps 5, 6, and 7, which will simplify through HO_2 steady state approximation:

$$\omega_{4f} = \omega_{5f} + \omega_{6f} + \omega_{7f}, \tag{26}$$

yielding

$$C_{\mathrm{HO_2}} = \frac{l_4 C_{\mathrm{H}}}{(k_{5f} + k_{6f})C_{\mathrm{H}} + k_{7f} C_{\mathrm{OH}}}, \tag{27}$$

In the above expression, C_{OH} may be replaced by its expression arising from H and OH steady states expressions from [11]

$$C_{\mathrm{HO_2}} = \frac{l_4}{k_{5f} + k_{6f} + k_{7f}\gamma_3 \frac{G}{2}}, \tag{28}$$

with $\gamma_3 = \frac{l_{3b}}{l_{3f}}$ and

$$G = 1 + \frac{l_4}{l_{3b}} - \frac{f}{\gamma_3} + \sqrt{\left(1 + \frac{l_4}{l_{3b}} + \frac{f}{\gamma_3}\right)^2 + 4\frac{f}{\gamma_3}\frac{l_4}{l_{3b}}}$$

$$f = \frac{k_{5f} + k_{6f}}{k_{7f}}$$

Note that only here, in estimating HO_2 steady-state concentration, will H and OH steady-state approximations be used. Reinjecting now the HO_2 steady-state expression into the H, O and OH production rates yields

$$\begin{cases} \dot{C_{\mathrm{H}}} & = -\omega_{1f} + \omega_{2f} + \omega_{3f} - \omega_{4f} - \omega_{5f} - \omega_{6f} \\ \dot{C_{\mathrm{O}}} & = \omega_{1f} - \omega_{2f} \\ \dot{C_{\mathrm{OH}}} & = \omega_{1f} + \omega_{2f} + \omega_{3f} + 2\omega_{5f} - \omega_{7f} \end{cases} \tag{29}$$

The joint evolution for H, O and OH radicals may therefore be described as

$$\frac{\mathrm{d}\bar{C}}{\mathrm{d}t} = \mathbf{A}\bar{C}, \tag{30}$$

where $\bar{C} = [C_{\mathrm{H}}, C_{\mathrm{O}}, C_{\mathrm{OH}}]^{\dagger}$ is the vector of radical concentrations, and $\mathbf{A}$ the associated Jacobian (inverse time units)

$$\mathbf{A} = \begin{bmatrix} -l_1 - l_4(2 - \mathcal{L}_7) & l_2 & l_{3f} \\ l_1 & -l_2 & 0 \\ l_1 + l_4(2\mathcal{L}_5 - \mathcal{L}_7) & l_2 & -l_{3f} \end{bmatrix}, \tag{31}$$

with

$$\mathcal{L}_5 = \frac{k_{5f}}{k_{5f} + k_{6f} + \gamma_3 k_{7f}\frac{G}{2}}, \quad \text{and} \quad \mathcal{L}_7 = \frac{\gamma_3 k_{7f}\frac{G}{2}}{k_{5f} + k_{6f} + \gamma_3 k_{7f}\frac{G}{2}}. \tag{32}$$

By summing the first line, second line twice and third line, it is clear that the crossover temperature, T_c, (for which the matrix becomes singular) satisfies $\alpha = 1$ with

$$\alpha = l_1/l_4 + \mathcal{L}_5, \tag{33}$$

in accordance with both limiting Eqs. (24, 25), and with previous studies [11]. As in [23] a simple expression for the quickly dominant largest eigenvalue can be derived by neglecting the third-order term of the characteristic polynomial

$$\lambda = \frac{2b_0}{\sqrt{b_1^2 + 4b_0 b_2} + b_1} \tag{34}$$

where

$$\begin{cases} b_0 &= 2l_2 l_3 l_4(\alpha - 1) \\ b_1 &= l_2[l_3 + l_4(2 - \mathcal{L}_7)] + 2l_3 l_4(1 - \mathcal{L}_5) \\ b_2 &= l_1 + l_2 + l_3 + l_4(2 - \mathcal{L}_7) \end{cases} \tag{35}$$

The eigenvalue λ in the lean and rich limits can be derived as

$$\lambda = \begin{cases} \lambda_l &= (\alpha - 1)\frac{\sqrt{2l_2 l_3}}{2 + \frac{l_1}{l_4}} \quad \text{in the lean limit,} \\ \lambda_r &= (\alpha - 1)\, 2l_4 \quad \text{in the rich limit.} \end{cases} \tag{36}$$

It can be observed that these two limits appear in the reaction rates of Eq. (23), which were found in [11] assuming H/O/OH steady states. Let us now rewrite the global reaction rate as

$$\omega = \lambda\zeta, \tag{37}$$

with λ being an inverse characteristic time, representative of the joint H/O/OH chain-branched explosion, and ζ a concentration accounting for the intermediate species growth.

By combining (23), (36) and (37), it becomes clear that the appropriate limits of ζ should be

$$\zeta = \begin{cases} \zeta_l & = \frac{\sqrt{l_2 l_3/2}}{k_{1b}} \frac{l_1+2l_4}{l_{3b}+l_4} \quad \text{in the lean limit} \\ \zeta_r & = \frac{1}{2}\frac{l_4}{k_8\gamma_3+k_9} \quad \text{in the rich limit} \end{cases} \tag{38}$$

in order to recover (23) in both lean and rich limits.

As for autoignition [6, 23, 24], assuming O/OH steady states in assessing the chain-branching characteristic time is a poor approximation, and using the continuous λ formulation yields a much better representation of the H/O/OH relative growth pathways with respect to the equivalence ratio.

Finally, we propose to unify the two limiting formulas for ζ as a geometric average

$$1/\zeta = \sqrt{\frac{1}{\zeta_\mathrm{l}^{\,2}} + \frac{1}{\zeta_\mathrm{r}^{\,2}}}, \tag{39}$$

and use $\omega = \lambda\zeta$ as global reaction rate for the global reaction (20). Note that the choice of geometric average is empirical, being the one yielding the best results through a series of tests.

2.3. Validations for premixed flames

Figure 2 compares burning-velocity results obtained with the present 1-step mechanism with those obtained from the detailed-chemistry description [25] and from a prior 1-step mechanism [11] for two different pressures. Cor-

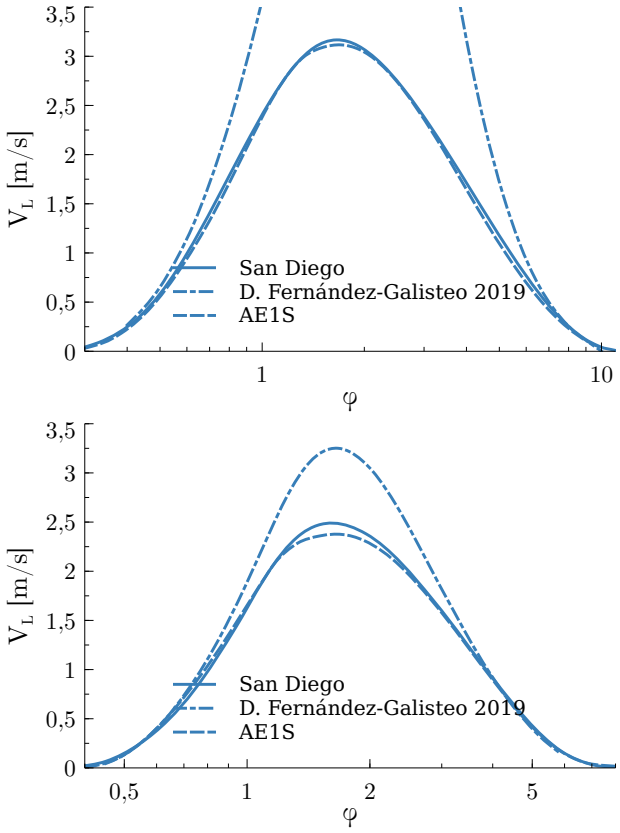

Figure 2: Laminar flame propagation speed for H_2-air mixtures at initial temperature of $T^0 = 300$K and pressure $P = 1$bar (top) and $P = 10$bar (bottom).

responding results for isentropic compression from 1 bar to $P_0 = 20$bar are shown in Fig. 3, which provides better agreement with detailed chemistry than the alternative found in the literature as the 3-step mechanism [6].

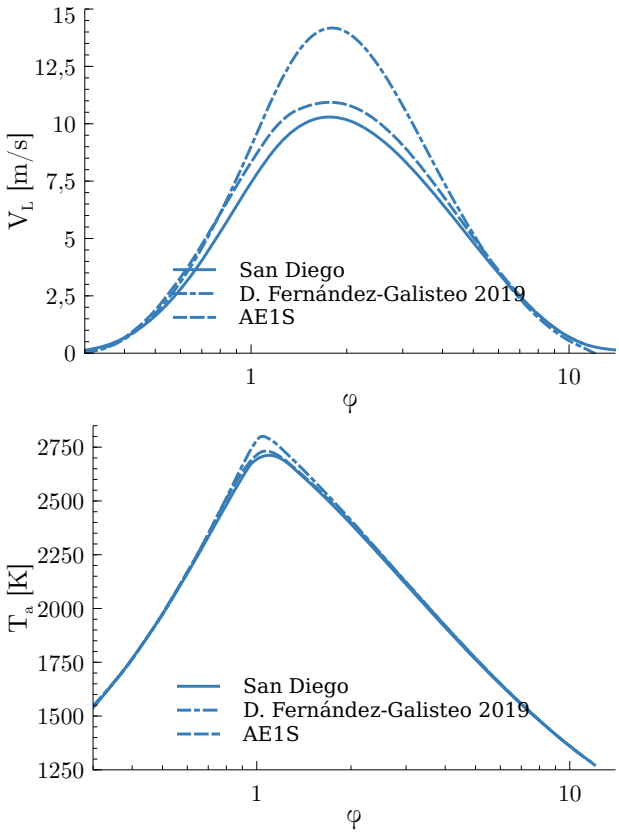

Figure 3: Laminar flame propagation speed (top) and adiabatic flame temperature (bottom) for an isentropic compression of H_2-air mixture at initial pressure and temperature of $P = 20$bar $T_0 = 706K$, respectively.

The non-monotonic pressure dependence of the burning rate has been tested in Fig. 4 for different He and Ar dilutions. The agreement is seen to be reasonable. Note however that available detailed mechanisms do not behave equally for this pressure dependence [26]. Results may therefore be improved by selecting rates from another mechanism, as the present model explicitly depends on them.

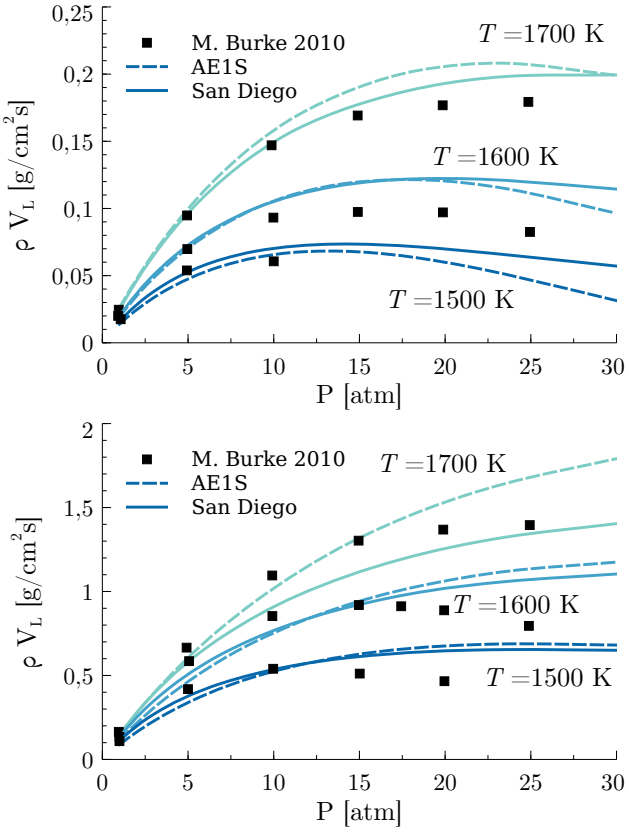

Figure 4: Pressure dependence of mass burning rates, ρV_L, for stoichiometric $H_2/O_2/He$ flames (top plot) and $H_2/O_2/Ar$ flames at equivalence ratio $\phi = 2.5$ for various flame temperatures T. Markers represent experimental data from [26].

3. Coupling with the ignition delay time

The present formulation has shown good accuracy in reproducing V_L, however, some practical situations need to fit more than one kinetic property at the same time. Taking a look at turbulent lifted flames [27], correct prediction flame structure requires that both, V_L and τ_{ig}, be satisfied by the chemical scheme. Chemical characteristics time for autoignition phenomena are very different from those of laminar flames and taking both properties with a single-step mechanism is non-trivial. Although many alternatives appear in the literature, e.g. switching between mechanisms based on the tracked initial temperature or local temperature, in the present work we will make use of the strategy developed in [19]. Ignition phenomena can be represented by a set of chain-branching reactions that build up a radical pool of precursors, η. When η concentration is high enough it will trigger the heat-release reactions. In this context, η will play the role of an efficiency variable on the heat release reaction that will be modeled as

$$\omega = \lambda\zeta \min\left(\frac{\eta}{\beta}, 1\right) \tag{40}$$

where β, settled to 4 in the present work, is a constant that represents a threshold for the η concentration in ω, related to the induction time definition [27]. The ignition precursor has the advantage of being passive in the sense that it does not enter into mass or energy balances but still needs to follow a classical advection-diffusion-reaction equation as

$$\frac{\partial \rho\eta}{\partial t} + \frac{\partial \rho v_\alpha \eta}{\partial x_\alpha} = \frac{\partial}{\partial x_\alpha}\left(D_\eta \frac{\partial \eta}{\partial x_\alpha}\right) + \omega_\eta, \tag{41}$$

where the Lewis number can be case-dependent or based on the molecular composition of the radical pool [28]. The problem is closed with the proper

model for ω_η. In the present work, the new model for hazardous ignition proposed by M. le Boursicaud et al. [28] has been employed. The reaction rate is modeled by an initiation-branching source term as

$$\omega_\eta = \lambda_\eta \eta + \epsilon \tag{42}$$

where ϵ is the initiation term and λ_η is the dominant eigenvalue of the Jacobian chain-branching chemistry. For simplicity and completeness, expressions of λ_η and ϵ have been summarized in the Supplemental Material. Although η does not play a role once a premixed flame is established, to avoid its exponential growth up to infinity, η has been clipped to 2β.

In figure 5 predictions of τ_{ig} for the present formulation have been compared with detailed chemistry computations. In the same figure, characteristics results of τ_{ig}, when η correction is not included, were also included. It can be seen how the ignition model recovers autoignition times as well as reference chemistry when the initial temperature is higher than the crossover temperature, equation (33). However, as the global reaction rate (37) becomes 0 when $T^0 \leq T_c$; ignition delay times tend to infinity. In practice, we expect most practical ignition events to occur above the flame crossover T_c as it is significantly smaller than the ignition crossover temperature [24]. Should it be required, a simple fix is nonetheless provided in the Supplementary Material.

4. Counterflow flames

Even though the present chemical scheme was developed for freely propagating premixed combustion, in partially premixed combustors flames are

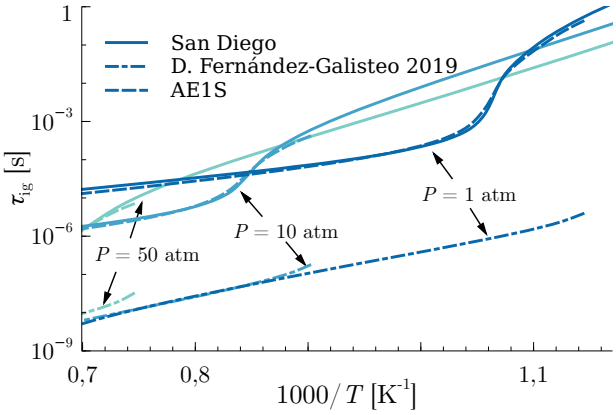

Figure 5: Ignition delay times for stoichiometric H_2-air mixtures at pressures $P = (1, 10, 50)$ bar.

subject to strain and local diffusion flame may appear as a consequence of the flow configuration. In that sense, following the steps done in [12], the mechanism will be tested in strained flame configurations. A one-dimensional counterflow configuration was employed to investigate twin-premixed and non-premixed flames at atmospheric ($p = 1$bar) and high-pressure conditions ($p = 25$bar).

Figures 6 and 7 show the maximum flame temperature versus the strain rate, defined in [29], for different pressures and fuel dilution ratios (X_{H_2}). In the figures, detailed chemistry computations were compared with results obtained using the reduced 1-step mechanism [11] and the present scheme.

It can be shown that the present scheme produces a better agreement with the reference mechanism for both, temperature and strain rate at the extinction conditions. It can be appreciated that when strain tends to zero, the proposed 1-step mechanism, produces excellent temperature predictions, thanks to the asymptotic analysis of the equilibrium composition. The

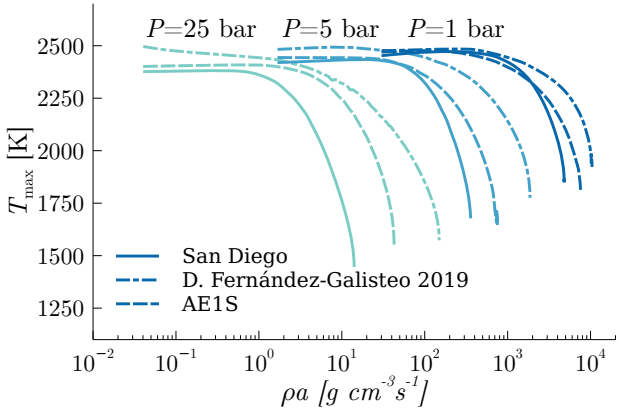

Figure 6: Maximum flame temperature of a stoichiometric H_2-air twin premixed counterflow flame versus the strain rate at ambient temperature $T^0 = 300$K.

error committed at extinction conditions is mainly related to the discrepancies in the flame thickness predictions [12] (e.g. the value obtained by the AE1S mechanism is 3.3 times smaller than the reference mechanism for atmospheric stoichiometric flames). This could be corrected by any classical flame thickening factor as those employed in turbulent flames [30]. When it is applied, the relative discrepancies are reduced by a factor of 10 for atmospheric premixed and diffusion flames.

5. Conclusions

A new single-step mechanism, built from an analytical description of the thermochemical equilibrium, is proposed for H_2 combustion. The mechanism follows the same philosophical lines as our recent contribution on hydrocarbon combustion [19], with the notable difference of being fully analytical. It can therefore be readily adapted to other detailed chemistry descriptions by substituting the adequate elementary rates. The mechanism may also be

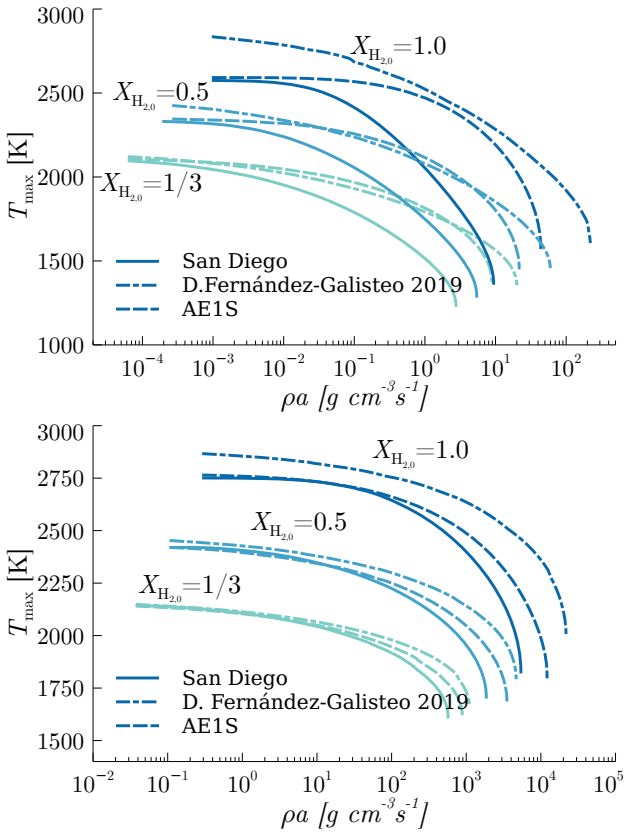

Figure 7: Maximum flame temperature of a N_2-H_2/air counterflow diffusion flame versus the strain rate at ambient temperature $T^0 = 300$K and pressure $P = 1$bar (top), $P = 25$bar (bottom).

used in conjunction with a separate detailed or reduced description for NOx chemistry.

The mechanism was validated over a wide range of pressure, temperature, and equivalence ratios for adiabatic flame temperatures and laminar premixed flame velocities. The 1-step formalism leads to trivial boundedness and low stiffness integration at the expense of intermediate-radical peaks in the flame structure.

Coupling with an ignition precursor formulation resulted in a global two-step mechanism able to reproduce flame propagation and autoignition events. The second step involves a passive scalar advection-diffusion-reaction equation that reproduces the chain-branched ignition process. This approach results in excellent induction time estimations without compromising the V_L predictions or the chemical integration stiffness.

Additionally, the mechanism was validated in strained premixed and diffusion flame extinction over a wide range of pressure and equivalence ratios. Later studies will validate the description's accuracy for turbulent reactive flows and deflagration-detonation transitions.

Acknowledgements

Forman Williams is gratefully acknowledged for his valuable input on the model and Marc Le Boursicaud is gratefully acknowledged for the fruitful conversations about the hydrogen hazardous ignition model [28]. A. Millán-Merino acknowledges support from the Margarita Salas postdoctoral grants funded by the Spanish "Ministerio de Ciencia, Innovación y Universidades" with Next Generation European Union through the "Convocatoria

de la Universidad Carlos III de Madrid de Ayudas para la recualificación del sistema universitario español para 2021-2023, de 1 de julio de 2021" TED2021-129446B-C43 funded by MCIN/AEI / 10.13039 / 501100011033 and European Union NextGenerationEU/ PRTR..

6. Supplementary material

For the sake of simplicity and completeness, expressions of λ_η and ϵ_η from M. le Boursicaud et al. [28] have been summarized in the Supplementary Material. The sources for the present work are available as Supplementary material and online at [31, 32], in a Cantera-compatible format.

References

[1] F. Mauss, N. Peters, B. Rogg, F. Williams, Reduced kinetic mechanisms for premixed hydrogen flames, in: N. Peters, B. Rogg (Eds.), Reduced Kinetic Mechanisms for Applications in Combustion Systems, Springer, 1993, pp. 29–43.

[2] E. Gutheil, G. Balakrishnan, F. Williams, Structure and extinction of hydrogen-air diffusion flames, in: N. Peters, B. Rogg (Eds.), Reduced Kinetic Mechanisms for Applications in Combustion Systems, Springer, 1993, pp. 177–195.

[3] K. Seshadri, N. Peters, F. Williams, Asymptotic analyses of stoichiometric and lean hydrogen-air flames, Combust. Flame 96 (1994) 407–427.

[4] G. Balakrishnan, M. Smooke, F. Williams, A numerical investigation of extinction and ignition limits in laminar nonpremixed counterflow-

ing hydrogen-air streams for both elementary and reduced chemistry, Combust. Flame 102 (1995) 329–340.

[5] F. A. Williams, Detailed and reduced chemistry for hydrogen autoignition, J. Loss Prevent. Proc. 21 (2008) 131–135.

[6] P. Boivin, C. Jiménez, A. L. Sánchez, F. A. Williams, An explicit reduced mechanism for H_2–air combustion, Proc. Combust. Inst. 33 (2011) 517–523.

[7] P. Boivin, A. L. Sánchez, F. A. Williams, Four-step and three-step systematically reduced chemistry for wide-range H_2–air combustion problems, Combust. Flame 160 (2013) 76–82.

[8] A. Abdelsamie, G. Lartigue, C. E. Frouzakis, D. Thévenin, The taylor-green vortex as a benchmark for high-fidelity combustion simulations using low-mach solvers, Comput. Fluids 223 (2021) 104935.

[9] P. C. Nassini, A. Andreini, M. D. Bohon, Characterization of refill region and mixing state immediately ahead of a hydrogen-air rotating detonation using les, Combust. Flame 258 (2023) 113050.

[10] D. Fernández-Galisteo, A. Sánchez, A. Liñán, F. Williams, One-step reduced kinetics for lean hydrogen–air deflagration, Combust. Flame 156 (2009) 985–996.

[11] D. Fernández-Galisteo, A. Weiss, A. L. Sánchez, F. A. Williams, A one-step reduced mechanism for near-limit hydrogen combustion with general stoichiometry, Combust. Flame 208 (2019) 1–4.

[12] J. Carpio, B. Li, D. Fernández-Galisteo, A. L. Sánchez, F. A. Williams, Systematically derived one-step kinetics for hydrogen-air gas-turbine combustion, Combust. Flame 250 (2023) 112633.

[13] T. P. Coffee, A. J. Kotlar, M. S. Miller, The overall reaction concept in premixed, laminar, steady-state flames. i. stoichiometries, Combust. Flame 54 (1983) 155–169.

[14] N. Marinov, C. Westbrook, W. Pitz, Detailed and global chemical kinetics model for hydrogen, in: S.H. Chan (Ed.), Transport Phenomena in Combustion, Taylor and Francis Group: Abingdon, UK, 1996, pp. 118–129.

[15] C. Wang, J. Wen, S. Lu, J. Guo, Single-step chemistry model and transport coefficient model for hydrogen combustion, SSci. China Technol. Sc. 55 (2012) 2163–2168.

[16] H. Y. Kim, N. I. Kim, Optimized global reaction mechanisms for h2, co, ch4, and their mixtures, Int. J. Hydrogen Energy 48 (2023) 24101–24112.

[17] B. Wang, W. Wei, S. Ma, G. Wei, Construction of one-step h2/o2 reaction mechanism for predicting ignition and its application in simulation of supersonic combustion, Int. J. Hydrogen Energy 41 (2016) 19191–19206.

[18] F. G. Schiavone, N. Detomaso, M. Torresi, D. Laera, An arrhenius-based one-step reaction mechanism for hydrogen-air flames simulations in an extended range of operating conditions, Int. J. Hydrogen Energy 57 (2024) 1229–1243.

[19] A. Millán-Merino, S. Taileb, P. Boivin, A new method for systematic 1-step chemistry reduction applied to hydrocarbon combustion, Proc. Combust. Inst. 39 (2023) 745–753.

[20] A. L. Sánchez, F. A. Williams, Recent advances in understanding of flammability characteristics of hydrogen, Prog. Energy Combust. 41 (2014) 1–55.

[21] E. Fernández-Tarrazo, A. L. Sánchez, A. Linan, F. A. Williams, A simple one-step chemistry model for partially premixed hydrocarbon combustion, Combust. Flame 147 (2006) 32–38.

[22] B. Franzelli, E. Riber, M. Sanjosé, T. Poinsot, A two-step chemical scheme for kerosene–air premixed flames, Combust. Flame 157 (2010) 1364–1373.

[23] P. Boivin, F. A. Williams, Extension of a wide-range three-step hydrogen mechanism to syngas, Combust. Flame 196 (2018) 85 – 87.

[24] P. Boivin, M. Le Boursicaud, A. Millan-Merino, S. Taileb, J. Melguizo-Gavilanes, F. A. Williams, Hydrogen ignition and safety, in: E. Tingas (Ed), Hydrogen for future thermal engines, Springer, 2023, pp. 161–236.

[25] Chemical-Kinetic Mechanisms for Combustion Applications, web.eng.ucsd.edu/mae/groups/combustion/mechanism.html, v. 2016-12-14.

[26] M. P. Burke, M. Chaos, F. L. Dryer, Y. Ju, Negative pressure dependence of mass burning rates of h2/co/o2/diluent flames at low flame temperatures, Combust. Flame 157 (2010) 618–631.

[27] S. Taileb, A. Millán-Merino, S. Zhao, P. Boivin, Lattice-boltzmann modeling of lifted hydrogen jet flames: A new model for hazardous ignition prediction, Combust. Flame 245 (2022) 112317.

[28] M. Le Boursicaud, S. Zhao, J.-L. Consalvi, P. Boivin, An improved passive scalar model for hydrogen hazardous ignition prediction, Combust. Flame 256 (2023) 112938.

[29] K. Seshadri, F. Williams, Laminar flow between parallel plates with injection of a reactant at high reynolds number, Int. J. Heat Mass Tran. 21 (1978) 251–253.

[30] T. Poinsot, D. Veynante, Theoretical and numerical combustion, RT Edwards, Inc., 2005.

[31] Universidad Politécnica de Madrid, Combustion group web page, `https://blogs.upm.es/labcmf`, accessed 20-02-2024.

[32] Alejandro Millan Merino, Personal gitlab repository: Cantera–Yosoytullamita, `https://gitlab.com/almillan/cantera-yosoytullamita`, accessed 20-02-2024.